Available online at www.sciencedirect.com

ScienceDirect

Ceramics International 42 (2016) 4837–4844

CERAMICS INTERNATIONAL

www.elsevier.com/locate/ceramint

Photoluminescence emission in zirconium-doped calcium copper titanate powders

F. Moura[a,1], A.C. Cabral[a], L.S.R. Rocha[b,*], E.C. Aguiar[c,2], A.Z. Simões[b,*], E. Longo[c,2]

[a]*Laboratório Interdisciplinar de materiais Avançados Universidade Federal de Itajubá- Unifei-Campus Itabira, Rua São Paulo 377, Bairro Amazonas, P.O. Box 355, 35900-37 Itabira, Minas Gerais, Brazil*

[b]*Universidade Estadual Paulista- Unesp – Faculdade de Engenharia de Guaratinguetá, Av. Dr Ariberto Pereira da Cunha 333, Bairro Pedregulho, P.O. Box 355, 12.516-410 Guaratinguetá, São Paulo, Brazil*

[c]*Laboratório Interdisciplinar em Cerâmica, Instituto de Química, Universidade Estadual Paulista, P.O. Box 355, 14801-907 Araraquara, São Paulo, Brazil*

Received 17 June 2015; received in revised form 26 November 2015; accepted 28 November 2015
Available online 4 December 2015

Abstract

Intense photoluminescence (PL) emission was observed in Zr-doped calcium copper titanate powders. The compounds were synthesized by a soft chemical method and heat treated at temperatures between 300 and 850 °C. The decomposition of the precursors was examined by X-ray diffraction, Fourier transform infrared, Fourier transform Raman, and ultraviolet–visible spectroscopies; as well as PL analysis. Here, we discuss the role of the structural ordering, which facilitates the self-trapping of electrons and charge transfer, and review the mechanism that triggers the PL. The most intense PL emission was obtained for the sample with 5% Zr calcined at 750 °C, which is neither highly disordered nor completely ordered at ~520 nm.

Keywords: A. Powders: chemical preparation; B. Electron microscopy; D. Perovskites

1. Introduction

The photoluminescence (PL) emissions of perovskite materials are closely related to the crystal structure and are caused by disorders in metal–oxygen polyhedra [1–12]. In particular, the TiO_6 octahedron has a remarkable structural flexibility. Under ambient conditions, such a characteristic is confirmed in many titanates by the presence of structures with lower symmetries, which are derived from the cubic aristotype structure (Pm3m symmetry) through the rotation or tilting of a regular rigid octahedron, or are due to the presence of distorted TiO_6 octahedra [13]. Despite the distorted structure, the rotation or tilting does not disrupt the corner-sharing connectivity. Furthermore, the tilt of the octahedral framework plays a key role in determining the properties of perovskite oxides.

Solution-based methods have been widely used to prepare ceramics [14,15]. The most adopted techniques can be grouped into four categories: (1) sol–gel processes; (2) metallorganic decompositions; (3) colloidal sol–gel processes; and (4) gel routes involving the formation of an organic polymeric complex (polymeric precursor method, PPM). The PPM can be divided into two groups [16]: (1) in situ polymerization of organometallic monomers; (2) preparation of a viscous solution system consisting of metal ions, polymers, and a solvent. At high polymer concentrations, this viscous solution can be easily converted into a thermoplastic gel. The in situ PPM has been extensively used to obtain ceramic powders with small particle sizes and a single phase [17]. This method was originally developed by Pechini [18], and is based on the chelation of a metallic cation by a carboxylic acid (such as citric acid) with further polymerization, promoted by the addition of ethylene glycol, and consequent polyesterification.

*Corresponding authors. Tel.: +55 12 3123 2765; fax: +55 12 3123 2800.
E-mail address: alezipo@yahoo.com (A.Z. Simões).
[1]Tel.: +55 31 3834 6472; fax: +55 31 3834 6136.
[2]Tel.: +55 16 3301 6643; fax: +55 16 3301 6692.

http://dx.doi.org/10.1016/j.ceramint.2015.11.169
0272-8842/

The properties of calcium copper titanate oxides (CCTO) are strongly dependent on the processing conditions [19], and doping [20,21]. For the doping effects, there are examples showing that the substitution of Ti for Zr [22,23] causes a decrease of an order of magnitude in the dielectric constant, also weakening the temperature dependence. Zr-doped calcium copper titanate (CCTZO) generally exhibits a fine-grained and dense microstructure, in which the Zr doping enhances the grain size uniformity [24]. Another interesting property is related to the PL, which is produced by the decay of excited electrons to their fundamental state. According to Pontes et al. [25], the PL signal is related to the structure, and fades away as the system shifts toward increased organization, indicating that the PL of CCTO/CCTZO powders originates from inorganic amorphous phases. However, up to certain quantities of dopants, some rearrangements occurring in the structure significantly enhance the PL emission. Thus, the PL behavior at room temperature can be related to the degree of order in the CCTO lattice, controlled by the $[TiO_5]$ and $[TiO_6]$ clusters. In a previous study, our group investigated the influence of the annealing temperature on the PL of CCTO powders [26]. In the current work, CCTZO powders were prepared with the aim of improving the lattice defects and phase transformations as well as increasing the surface area, which affects the crystallization process of the main phase. CCTO/CCTZO powders were obtained at low calcination temperatures affecting the PL behavior. In the framework of a more extensive project [27–29] aimed at the design and synthesis of perovskite-based materials with PL properties, the influence of the degree of order on the structural and PL behavior of CCTO/CCTZO powders has been investigated. Therefore, the novelty of this research lies in the examination of the impact of the structural order and disorders associated with Zr doping on the PL emission. Four main critical steps are involved: (1) synthesis of the powders; (2) structural characterization of the disorders to clarify their relationships with the orderliness of the parental samples; (3) identification of the formation mechanisms of the disorders; (4) understanding of the critical relationship between the structural degree of order and disorders and the PL properties.

2. Experimental procedure

Powders were synthesized by the PPM. Calcium carbonate ($C_{12}H_{28}O_4Ti$, Aldrich, 99.999%), titanium (IV) isopropoxide ($C_{12}H_{28}O_4Ti$, Aldrich, 99.999%), copper (II) carbonate basic ($CuCO_3 \cdot Cu \cdot (OH)_2$, Aldrich, 99.99%), zirconium hydroxide ($Zr(OH)_4$, IPEN 99.5%), ethylene glycol (99%, J.T. Baker), and anhydrous citric acid (99.5%, J.T Baker) were used as starting materials. Ti (IV) isopropoxide and Zr hydroxide were dissolved in aqueous solutions of citric acid under constant stirring at 50 °C. Subsequently, the Ca and Cu precursors were added, and the citrate solution was stirred at 95 °C to obtain a clear and homogenous solution. After homogenization, ethylene glycol was added to promote the citrate polymerization. The metal: citric acid:ethylene glycol ratio was fixed at 1:4:16. The polymeric resin was placed in a conventional furnace and heat treated at 300 °C for 4 h, forming the precursor powders. These were then heat treated at temperatures between 300 and 850 °C for 2 h in a tube furnace under ambient conditions, as reported in the literature [30]. The samples are referred to as CCTO, CCTO:5Zr, CCTO:10Zr, and CCTO:15Zr, based on the amount of Zr in the material. The crystalline phase of the powders was analyzed using X-ray diffraction (XRD; Rigaku-DMax 2500PC, Japan) with Cu-Kα radiation in the 2θ range of 20–80° and a rate of $0.03^\circ\ min^{-1}$. Fourier transform Raman (FT-Raman) spectroscopy was performed on a Bruker – RFS 100 (Germany), with a 1064 nm Nd:YAG laser used as the excitation source with power of 70 mW. Ultraviolet–visible (UV–vis) spectroscopy of the powders was performed using Cary 5G equipment. The morphology of the as-prepared samples was observed using a high-resolution field-emission gun scanning electron microscope (FEG-SEM; Supra 35-VP, Carl Zeiss, Germany). The PL properties were measured with a Thermal Jarrel-Ash Monospec27 monochromator and a Hamamatsu R446 photomultiplier. The excitation source was a 350.7 nm krypton ion laser (Coherent Innova) operating at 200 mW. All measurements were performed at room temperature.

3. Results and discussion

Fig. 1a–d shows the evolution of the XRD patterns of the CCTO powders, heat treated at temperatures between 300 and 850 °C for 2 h under ambient conditions, containing different amounts of Zr. The diffraction peaks, visible even in the powders annealed at 300 °C, indicate that, at these temperatures, the powders begin to show long-range structural order, with CuO, TiO_2, and ZrO_2 phases clearly evident. The CCTO phase shows increasing structural order as the calcination temperature rises to 850 °C, in agreement with the literature data [31–33]. However, the CuO phase is suppressed in the CCTZO powder, which indicates that Zr doping can inhibit the decomposition of the CCTO organic material during the annealing, or even shift its crystallization temperature to higher values. Further increase in temperature leads to a single CCTO phase, with consequent complete loss of PL properties [26]. The crystallization process of the structurally disordered CCTO clearly starts at temperatures as low as 400 °C (see Fig. 1a) and is completed after annealing at 850 °C, allowing its partial indexation in accordance with the lattice parameter values obtained from the standard JCPDS no. 75-2188 data.

Fig. 2 shows the Raman spectra of CCTO and CCTZO powders heat-treated at 750 °C for 2 h under ambient conditions. Four modes associated with the CCTO phases can be observed at 296, 447, 501, and 605 cm^{-1}, in agreement with other reported results for CCTO [34]. The main mode, associated with TiO_2 (anatase phase), shows an intense signal at around 143 cm^{-1}, in agreement with the literature data [35]. In addition to the main modes of CCTO and TiO_2 phase, the 320 cm^{-1} peak, typical of the measurement system, is clearly seen in all samples [36]. The Raman mode at 296 cm^{-1} is a weak low-frequency mode, which is almost certainly associated with the E_g mode [37], and develops a broad shoulder as the Zr content increases, indicating possible short-range lattice

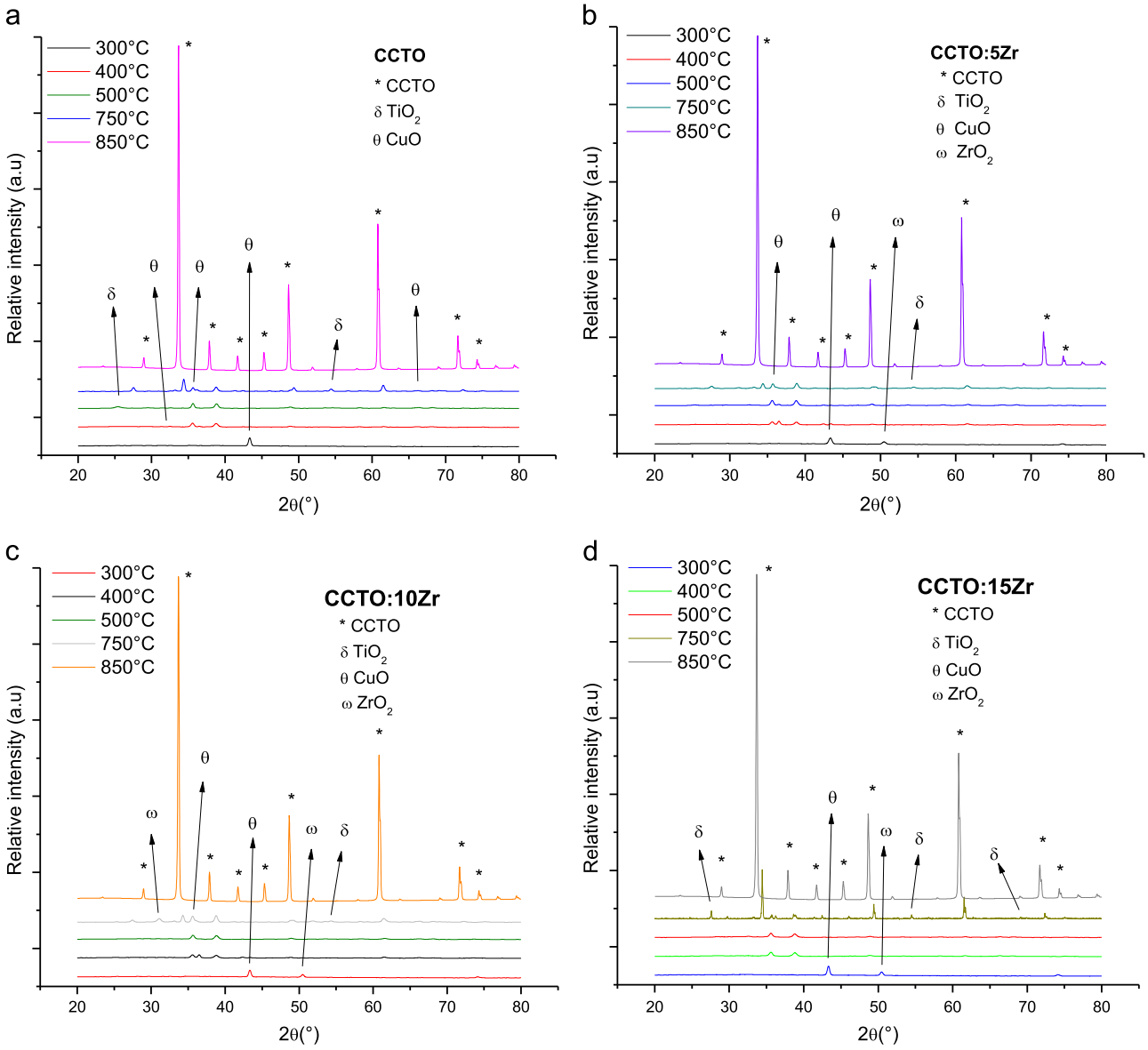

Fig. 1. X-ray diffraction patterns of calcium copper titanate (CCTO)/Zr-doped calcium copper titanate (CCTZO) powders heat treated at temperatures between 300 and 850 °C for 2 h under ambient conditions: (a) CCTO; (b) CCTO:5Zr; (c) CCTO:10Zr; (d) CCTO:15Zr.

distortions. The modes at 447 cm^{-1} and 501 cm^{-1} are associated with the A_g symmetry (TiO_6, rotation-like), while that at 605 cm^{-1} is related to the F_g symmetry (O–Ti–O, anti-tensing). A similar scenario, to the E_g mode, can be seen for the 447 cm^{-1} peak, which becomes broader as the amount of Zr increases, indicating its influence on the formation of the $[TiO_5]/[TiO_6]$ clusters. According to Kolev et al. [7] and Valim et al. [38], the modes near 290, 445, and 510 cm^{-1} are associated with TiO_6 rotation-like modes, whereas the modes at 574 cm^{-1} and ~780 cm^{-1} are characteristic of Ti–O–Ti vibrations (anti-tensing and tensing, respectively) of the TiO_6 octahedron. Although Raman spectroscopy is more sensitive than XRD, no traces of CuO, $CaTiO_3$ and ZrO_2 modes were observed, as reported in the literature [38]. This indicates that these phases are more soluble than TiO_2 in the CCTO lattice at short-range.

Fig. 3 illustrates the UV–vis spectral absorbance dependence of the disordered and partially ordered CCTO/CCTZO powders calcined at 300 °C and 750 °C, respectively. The maximum absorption is located at ~400 nm, and the respective band gap values were determined using the Kubelka model [39]. The optical energy band gap is related to the absorbance and photon energy as follows (1):

$$h\nu\alpha \propto (h^{\circ} - E_g^{opt})^2 \quad (1)$$

where α is the absorbance, h is the Planck constant, ν is the frequency, and E_g^{opt} is the optical band gap [40]. In partially ordered CCTO powders, the absorbance measurements suggested a non-uniform band gap structure with a tail of localized states (see Fig. 3a and b). These results were confirmed by the UV–vis spectra, which showed a decrease in the Urbach tail when the temperature increased. The reduction in the optical

band gap of the disordered CCTO as a function of the Zr content can be correlated with the raise of structural defects, or localized states, inside the band gap. This behavior indicates that the ZrO_6 octahedron is more distorted than the TiO_6 octahedron in the perovskite lattice. The values were between 1.68 and 2.48 eV for the disordered powders, obtained at 300 °C, and between 2.02 and 2.06 eV for the partially ordered powders, obtained at 750 °C. The optical band gaps were larger than those reported by Kant et al (~200 meV) [41], and for the system partially crystallized at 300 °C, the level of Zr doping had a significant influence on . The main changes in the band gap can be ascribed to a reduction of defects in the lattice, which results in the decrease of the intermediary energy levels due to the reduction of oxygen vacancies located in the BO_6^- octahedra. This behavior presumably occurs due to the distortions caused into the $[MO_6]$ octahedral group by different Zr contents, which induces more distortions, in the octahedron, than Ti atoms, as shown by Cavalcante et al. [42]. This behavior occurs due to the covalent nature of the bonds formed by these network formers (Ti and Zr), which results in a more important role for the structural organization and formation of the first coordination centers (TiO_6 and ZrO_6) in the lattice. However, displacements of the network modifiers (Ca and Cu), due to addition of Zr, results in great differences from the experimental value of the gap because these form bonds that are ionic in nature promoting disorder among the oxygens that are not linked to the lattice. The atoms act via the formation of second centers of coordination (CuO and CaO_2) in the lattice. In this way, the gaps are bigger when displacement of Zr atoms is promoted as this result in $[ZrO_6]$ clusters, which are more distorted than $[TiO_6]$ clusters. Furthermore, Laulhe´ et al. [43] showed through extended X-ray absorption fine structure measurement that fluctuations in the Zr–O distance can be due to Zr displacements in their octahedron, but can also result from distortions of the ZrO_6 octahedron induced by the Zr/Ti chemical disorder. The disordered powder (Fig. 3a) presents a spectral dependence similar to that observed in amorphous semiconductors such as silicon. The nature of these exponential optical edges and tails may be associated with localized defect states promoted by the disordered structure. In this sample, high absorbance values can be obtained throughout the whole photon energy range, due to the high number of secondary phases. The differences in the optical band gap behavior can be associated with the changes in the local atomic structure or lattice, as observed in the XRD and Raman results. However, the CCTO/CCTZO powders heat treated at 750 °C showed a typical interband transition in the high-energy region of the absorbance curve (Fig. 3b). The progressive treatment promotes a reduction of the structural disorder and an increase of the inclination of the dashed line or tail, reducing the deviations in the optical gap value. Therefore, the variation of the optical band gap as a function of the temperature can be used to evaluate the degree of structural order in CCTO and CCTZO powders prepared by the soft chemical method.

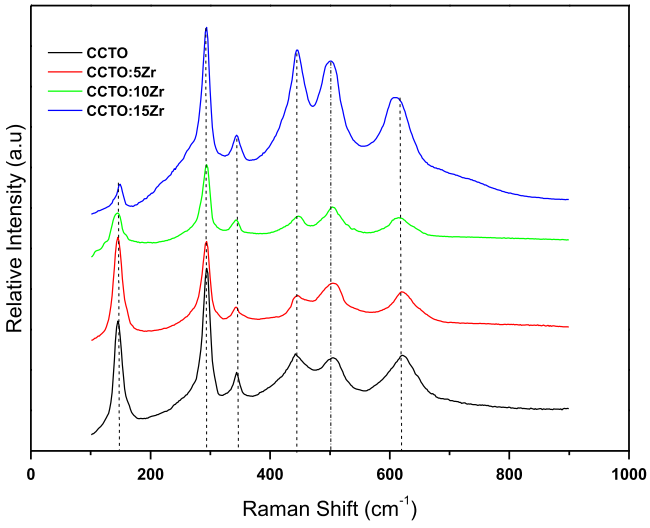

Fig. 2. Raman spectra of (CCTO)/(CCTZO) powders heat treated at 750 °C for 2 h under ambient conditions.

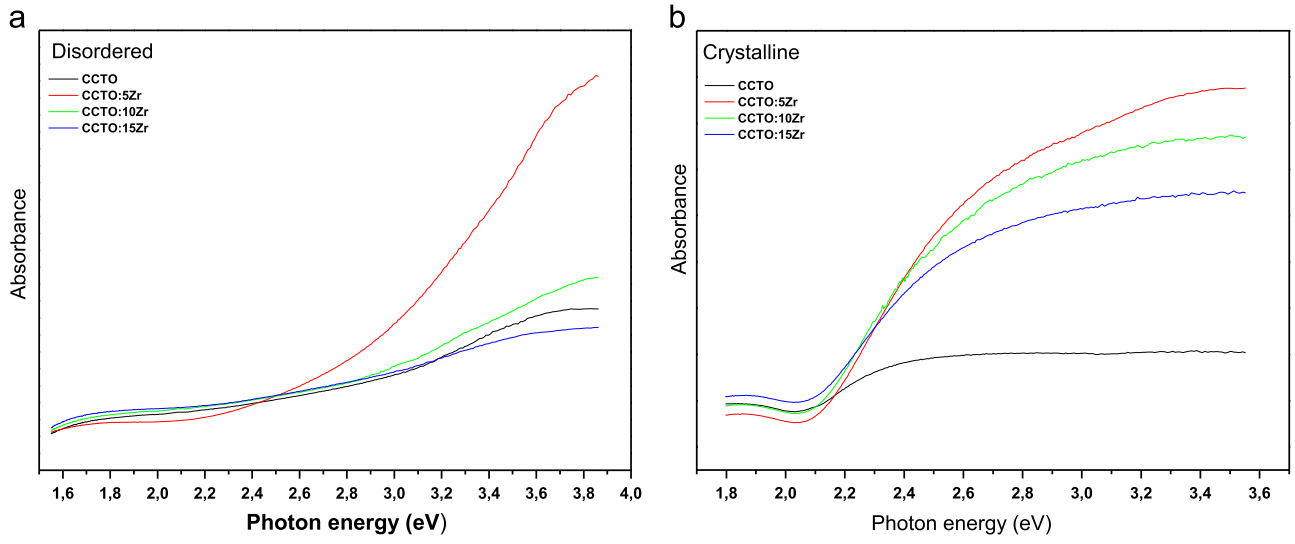

Fig. 3. Ultraviolet–visible absorbance spectra of (CCTO)/(CCTZO) powders heat treated at (a) 300 and (b) 750 °C for 2 h under ambient conditions.

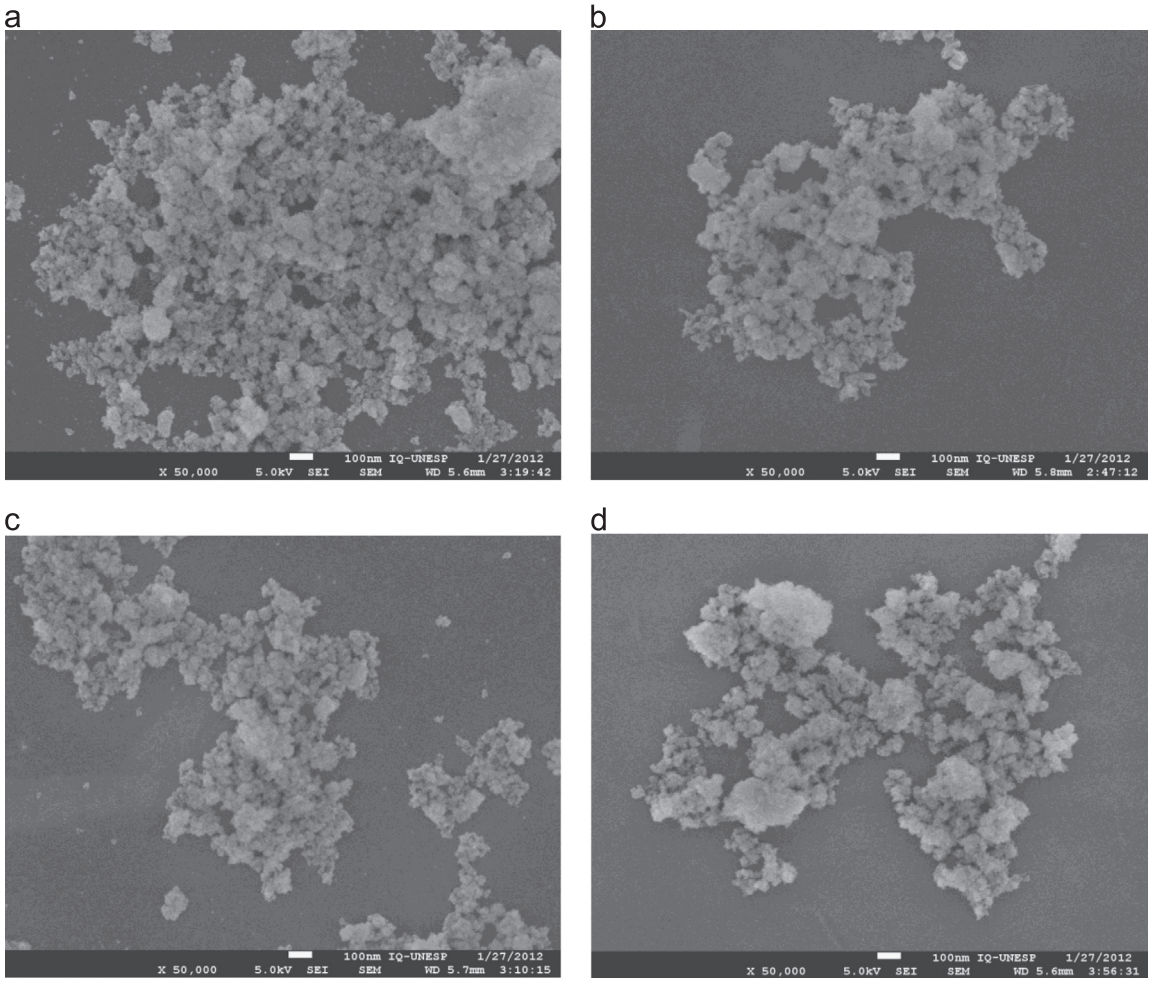

Fig. 4. Field-emission gun scanning electron microscopy images of (a) CCTO; (b) CCTO:5Zr; (c) CCTO:10Zr and (d) CCTO:15Zr powders heat treated at 750 °C for 2 h under ambient conditions.

FEG-SEM micrographs of CCTO (a) and CCTZO with different Zr contents (b–d) are shown in Fig. 4. There are clearly significant differences in the morphology of the CCTO and CCTZO powders. Poor contrast and intense agglomeration of extremely fine particles are observed in the CCTZO powders, while monodispersed particles with a lower degree of aggregation are observed in the undoped system. The higher agglomeration degree of CCTZO may be attributed to Zr doping, which can suppress the decomposition of organic material in CCTO during calcination at high temperature. As shown in Fig. 4a, the CCTO powder exhibited larger particle sizes with a better homogeneous distribution. However, as seen in Fig. 4b–d, upon increasing the Zr content, the CCTZO powders exhibited a higher degree of agglomeration due to the reduction of the particle dimensions. Therefore, the particle size of the CCTZO powders was reduced, and the uniformity vanished via Zr doping. Micrometric and anisotropic CCTZO agglomerates could be observed [44].

The evolution of the PL emissions for both CCTO and CCTZO powders obtained at 750 °C are shown in Fig. 5. Basically, the origin of the PL emission in the Zr-doped samples can be associated with the lattice symmetry breaking due to the presence of oxygen vacancies or distortions, and the

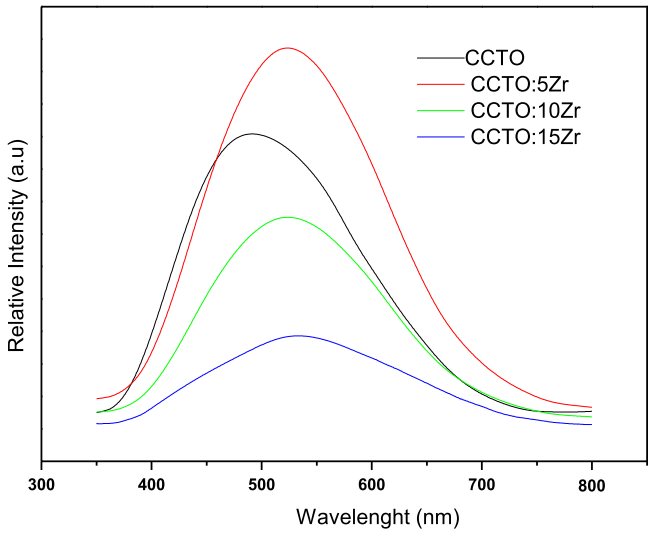

Fig. 5. Photoluminescence spectra at room temperature of (CCTO)/(CCTZO) powders heat treated at 750 °C for 2 h under ambient conditions.

charge transfer occurring from the $[TiO_5 \cdot V_o^{\bullet}] - [ZrO_5 \cdot V_o^{\bullet}]$ to the $[TiO_6]'$ clusters, which creates electrons and hole polarons that can be designed as Jahn–Teller bipolarons. The powder

calcined at 750 °C for 2 h was initially composed of the polymeric precursor, which exhibited low PL. However, after heating, the PL was likely associated with the level of structural organization [44] and the charge transfer occurring between Ca, Cu and Ti ions. Notably, there are electronic levels of the amorphous cluster included in the wide band gap of the crystalline cluster, demonstrating a charge transfer between (TiO_6) and (TiO_5) centers. In this case, a Ti ion forms an octahedral TiO_6 complex, while a second Ti ion, in a different octahedron, forms a TiO_5 complex plus an oxygen vacancy. If these two different $V_o^{\bullet\bullet}$ structures coexist, the charges of the two holes are compensated by one oxygen vacancy. This suggests that the formation of an amorphous cluster may introduce electronic levels in the forbidden gap. The octahedral geometry of the crystalline cluster is an advantage for TiO_6 because it minimizes the electrostatic interactions between the six oxygen ligands arranged around the positively charged (Ti (1)) center. The interactions between Ti and O in the TiO_6 complex are strong, whereas they are weak in the TiO_5 complex. This means that the d_z^2 and $d_{x^2}^{2-}$ bonding combinations in the crystalline cluster are unstable, in contrast to those in the amorphous cluster. Charge trapping is the most critical condition to obtain intense PL emission. Structural defects at short and intermediate ranges lead to the formation of intermediate energy levels in the band gap as well as inhomogeneous charge distributions in the unit cell, allowing electrons to be trapped. The lower conduction band (CB) is mainly formed by the 4d orbitals of Zr atoms. The levels responsible for the reduction of the band gap are mainly due to the 2p orbitals of oxygen atoms in the valence band (VB), stabilized by the break of the Zr–O bond. The localized levels are energetically distributed so that several photons are able to excite the trapped electrons. After photon excitation, a recombination process takes place, in which an electron of the CB loses its energy and reoccupies the energy level of an electron (e^-) or hole ($h^{\cdot}$) in the VB. The results showed that the charge transfer concerns not only the network former (TiO_6), but also the network modifiers (CaO_2 and CuO). Thus, the symmetry of the $CaTiO_3$ and $CuTiO_3$ systems is modified intrinsically by the random movement of the Ca and Cu atoms, due to their ionic character. The highest PL emission was originated from the CCTO:5Zr sample obtained at 750 °C, in which the structure was neither completely amorphous nor fully ordered. The structural transformations of the main phase start from the early stage of the polyesterification of the citrate solution containing the Ti, Ca and Cu ions [45]. Ti, which is the lattice former, ideally bonds with six oxygen atoms, but it can adopt various other coordination numbers before reaching this ideal configuration. Before crystallization, the structure is a mixture of TiO_x clusters intercalated by Ca, Cu, and Zr atoms. Upon crystallization, only TiO_6 clusters remains and the PL vanishes, showing that complete order quenches the PL emission. According to Pontes et al. [25], if the PL signal is related to the amorphous structure, the signal fades away as the system becomes increasingly organized. This is a good indication that the PL of CCTO and CCTZO powders obtained by the PPM, originates from inorganic amorphous phases with PL properties. CCTO treated at 750 °C presented an intense and broad PL with a maximum in the visible region at ~490 nm. The PL emission may be lower, owing to the presence of a large number of defects associated with disorder in the CCTO lattice. Interestingly, the CCTO powder thermally treated at 750 °C showed the main PL band with a maximum emission at around 490 nm (strong green emission) upon excitation by a 350.7 nm wavelength laser. This emission can be related to TiO_5, CuO_{11}, and CaO_{11} vacancy clusters, represented by $[CaO_{11} \cdot V_o^x]$, $[TiO_5 \cdot V_o^x]$, $[CuO_{11} \cdot V_o^x]$ and $[TiO_5 \cdot V_o^{\bullet\bullet}]$, in which $V_o^{\bullet\bullet}$ stands for oxygen vacancies. In fact, the PL emission process is related to defects or to the degree of order–disorder in the CCTO lattice, which can be attributed to the presence of $[TiO_6–TiO_5 . V_o^{\bullet}]$ or $[ZrO_6–ZrO_5 \cdot V_o\bullet]$ complex clusters [44,46]. TiO_6 would be linked to CaO_{12} and/or CuO_{12} clusters, which could also be associated with these complex clusters, respectively. These complex defects are deeply inserted into the band gap, leading to PL emission. A proposed model for wide band PL, based on the literature data, states that the most important effects occur before excitation, i.e., before the photon arrives. According to the Kroger–Vink notation [46], some complexes can create electron-captured oxygen vacancies:

$$\left[TiO_5 \cdot V_o^x\right] + [TiO_6]^x \rightarrow [TiO_5 \cdot V_o] + [TiO_6]' \quad (2)$$

$$[TiO_5 \cdot V_o] + [TiO_6]^x \rightarrow [TiO_5 \cdot V_o] + [TiO_6]' \quad (3)$$

$$[TiO_5 \cdot V_o] + \frac{1}{2}O2 \rightarrow [TiO_6]^x \quad (4)$$

$$[ZrO_5 \cdot V_o^x] + [ZrO_6]^x \rightarrow [ZrO_5 \cdot V_o] + [ZrO_6]' \quad (5)$$

$$[ZrO_5 \cdot V_o] + [ZrO_6]^x \rightarrow [ZrO_5 \cdot V_o] + [ZrO_6]' \quad (6)$$

$$[ZrO_5 \cdot V_o] + \frac{1}{2}O2 \rightarrow [ZrO_6]^x \quad (7)$$

In these structures, the $[TiO_5 \cdot V_o^x]$ and $[ZrO_5 \cdot V_o^x]$ clusters are donors, $[TiO_6]^x$ and

$[ZrO_6]^x$ clusters are acceptors, $[TiO_6]'$ and $[ZrO_6]$ clusters act as electron donors, complex vacancies as $[TiO_5 \cdot V_o^{\bullet}]$ and $[ZrO_5 \cdot V_o^{\bullet}]$ tend to trap electrons or holes, and $[TiO_5 \cdot V_o^{\bullet}]$ and $[ZrO_5 \cdot V_o^{\bullet}]$ act as electron traps. These equations suggest that the oxygen vacancy trapped electron in the VB is a necessary requirement for the transition of a VB electron to the CB, which results in PL emission as it returns to its fundamental state [47,48].

4. Conclusions

Pure and impurity-free Zr doped CCTO powders were synthesized by the soft chemical method at 850 °C for 2 h. The XRD analysis suggests that the powder crystallization process begins at 400 °C, reaching complete order at 850 °C. The Raman analysis revealed that, as the Zr content increases, the short-range lattice distortions of the perovskite structure become evident, influencing the formation of the $[TiO_5]/[TiO_6]$

clusters. The UV–vis spectra revealed the presence of localized energy levels in the band gap, possibly due to a certain structural disorder in the lattice. As the Zr content increased, the band gap energy decreased, owing to the presence of localized levels in the band gap and charge discontinuities induced by the local disorder, which favor the trapping of electrons and holes for PL emission. CCTO:5Zr powders heat treated at 750 °C for 2 h exhibited the highest PL, with an intense and broad maximum at ~520 nm and a strong emission at ~490 nm, which can be controlled by introducing complex defects into the band gap. Therefore, the mechanism responsible for the PL emission in such systems is a consequence of the charge transfer not only in the network former (TiO_6), but also in the network modifiers (CaO_2 and CuO) and the mixture of TiO_x clusters intercalated by Ca, Cu and Zr atoms in which TiO_6 is linked to CaO_{12} and/or CuO_{12} clusters, associated with $[CaO_{11} \cdot V_o^x]$, $[TiO_5 \cdot V_o^x]$, $[CuO_{11} \cdot V_o]$, and $[TiO_5 \cdot V_o^{\bullet\bullet}]$ clusters.

Acknowledgments

The financial support of this research project by the Brazilian research funding agencies CNPq FAPESP 2013/07296-2 and FAPEMIG is gratefully acknowledged.

References

[1] C.C. Homes, T. Vogt, S.M. Shapiro, S. Wakimoto, A.P. Ramirez, Optical response of high-dielectric-constant perovskite-related oxide, Science 293 (2001) 673–676.
[2] M.A. Subramanian, L. Dong, N. Duan, B.A. Reisner, A.W. Sleight, High dielectric constant in $ACu_3Ti_4O_{12}$ and $ACu_3Ti_3FeO_{12}$ phases, J. Solid State Chem. 151 (2000) 323–325.
[3] A.P. Ramirez, M.A. Subramanian, M. Gardel, G. Blumberg, D. Li, T. Vogt, S.M. Shapiro, Giant dielectric constant response in a copper-titanate, Solid State Commun. 115 (2000) 217–220.
[4] T.B. Adams, D.C. Sinclair, A.R. West, Giant barrier layer capacitance effects in $CaCu_3Ti_4O_{12}$, Ceram. Adv. Mater. 14 (2002) 1321–1323.
[5] A. Kotizsch, G. Blumberg, A. Gozar, B. Dennis, A.P. Ramirez, S. Trebst, S. Wakimoto, Antiferromagnetism in $CaCu_3Ti_4O_{12}$ studied by magnetic Raman spectroscopy, Phys. Rev. B 65 (2002) 0524061–0524064.
[6] L.X. He, J.B. Neaton, M.H. Cohen, D. Vanderbilt, First-principles study of the structure and lattice dielectric response of $CaCu_3Ti_4O_{12}$, Phys. Rev. B 65 (2002) 112–123.
[7] N. Kolev, R.P. Bontchev, A.J. Jacobson, V.N. Popov, V.G. Hadjiev, A.P. Litvinchuk, M.N. Iliev, Raman spectroscopy of $CaCu_3Ti_4O_{12}$, Phys. Rev. B 66 (2002) 102–106.
[8] P. Lunkenheimer, V. Bobnar, A.V. Pronin, A.I. Ritus, A.A. Volkov, A. Loidl, Origin of apparent colossal dielectric constants, Phys. Rev. B 66 (2002) 105–109.
[9] D.C. Sinclair, T.B. Adams, F.D. Morrison, A.R. West, $CaCu_3Ti_4O_{12}$: one-step internal barrier layer capacitor, Appl. Phys. Lett. 80 (2002) 153–156.
[10] L. Chen, C.L. Chen, Y. Lin, Y.B. Chen, X.H. Chen, R.P. Bontchev, C.Y. Park, A. Jacobson, High temperature electrical properties of highly epitaxial $CaCu_3Ti_4O_{12}$ thin films on (001) $LaAlO_3$, Appl. Phys. Lett. 82 (2003) 317–320.
[11] W. Cruz, E.M. Si, P.D. Johnson, P.W. Barnes, P. Woodward, A.P. Ramirez, Epitaxial thin films of the giant-dielectric-constant material $CaCu_3Ti_4O_{12}$ grown by pulsed-laser deposition, Appl. Phys. Lett. 81 (2002) 56–59.
[12] L. Fang, M.R. Shen, Deposition and dielectric properties of $CaCu_3Ti_4O_{12}$ thin films on Pt/Ti/SiO_2/Si substrates using pulsed-laser deposition, Thin Solid Films 440 (2003) 60–65.
[13] W.J. Lee, Y.M. Kim, H.G. Kim, Pt-base electrodes and effects on phase formations and electrical properties of high-dielectric thin films, Thin Solid Films 269 (1995) 75–79.
[14] N.G. Eror, H.U. Anderson, Polymeric precursors synthesis and processing of electronic materials in the BaO–TiO_2 system, J. Mater. Sci. 25 (1990) 1169–1183.
[15] S.G. Cho, P.F. Johnson, R.A. Condrate Sr, Thermal decomposition of (Sr, Ti) organic precursor during the Pechini process, J. Mater. Sci. 25 (1990) 4738–4744.
[16] S. Kumar, G.L. Messing, Synthesis of barium titanate by a basic pH Pechini process, in: Proceedings of the Material Research Society Symposium Proceedings, 271, 1992, pp. 95–100.
[17] M.P. Pechini, Method of Preparing Lead and Alkaline Earth Titanates and Niobates And Coating Method Using the Same to Form a Capacitor. U.S. Patent No 3 330 697, July 11, 1967.
[18] M. Liu, D. Wang, Synthesis of $La_{1-z}Sr_zCo_{1-y}Fe_yO_{3-y}$ on dense or porous substrates using the polymeric precursors method, J. Mater. Res. 10 (1995) 3210–3214.
[19] B.A. Bender, M.J. Pan, The effect of processing on the giant dielectric properties of $CaCu_3Ti_4O_{12}$, Mater. Sci. Eng. B. 117 (2005) 339–347.
[20] G. Chiodelli, V. Massarotti, D. Capsoni, M. Bini, C.B. Azzoni, M.C. Mozzati, P. Lupotto, Electric and dielectric properties of pure and doped $CaCu_3Ti_4O_{12}$ perovskite materials, Solid State Commun. 132 (2004) 241–246.
[21] D. Capsoni, M. Bini, V. Massarotti, G. Chiodelli, M.C. Mozzati, C.B. Azzoni, Role of doping and CuO segregation in improving the giant permittivity of $CaCuTi_4O_{12}$, J. Solid State Chem. 177 (2004) 4494–4500.
[22] E.A. Patterson, S. Kwon, C.-C. Huang, D.P. Cann, Effects of ZrO_2 additions on the dielectric properties of $CaCu_3Ti_4O_{12}$, Appl. Phys. Lett. 87 (2005) 182911–182913.
[23] J. You, Q. Chen, W. Ju, L. Li, K. Chen, Effects of the replacement of Ti by Zr on the dielectric properties of $CaCu_3Ti_4O_{12}$ ceramics, Key Eng. Mater. 368–372 (2008) 118–120.
[24] Q.G. Chi, L. Gaoa, X. Wanga, J.Q. Linb, J. Sunb, Q.Q. Lei, Effects of Zr doping on the microstructures and dielectric properties of $CaCu_3Ti_4O_{12}$ ceramics, J. Alloy. Compd. 559 (2013) 45–48.
[25] F.M. Pontes, C.D. Pinheiro, E. Longo, E.R. Leite, S.R. Lazaro, R. Magnani, P.S. Pizani, T.M. Boschi, F. Lanciotti, Theoretical and experimental study on the photoluminescence in $BaTiO_3$ amorphous thin films prepared by the chemical route, J. Lumin. 104 (2003) 175–185.
[26] F. Moura, A.Z. Simoes, R.C. Deus, M.R. Silva, J.A. Varela, E. Longo, Intense photoluminescence emission at room temperature in calcium copper titanate powders, Ceram. Int. 39 (2013) 3499–3506.
[27] K. Nakamoto, Infrared and Raman Spectra of Inorganic and Coordination Compounds, 4th ed., Wiley, New York, 1986, p. 386–388.
[28] A.Z. Simões, A. Ries, F.M. Filho, J.A. Varela, E. Longo, Fatigue-free behavior of $Bi_{3.25}La_{0.75}Ti_3O_{12}$ thin films grown on several bottom electrodes by the polymeric precursor method, Appl. Phys. Lett. 85 (2004) 5962–5965.
[29] A.Z. Simões, L.S. Cavalcante, C.S. Riccardi, J.A. Varela, E. Longo, Improvement of fatigue resistance on La modified $BiFeO_3$ thin films, Curr. Appl. Phys. 9 (2009) 520–523.
[30] F. Moura, A.Z. Simões, E.C. Aguiar, I.C. Nogueira, M.A. Zaghete, J.A. Varela, E. Longo, Dielectric investigations of vanadium modified barium zirconium titanate ceramics obtained from mixed oxide method, J. Alloy. Compd. 479 (2009) 280–283.
[31] C. Masingboon, S. Maensiri, T. Yamwong, P. Anderson, S. Seraphin, Nanocrystalline $CaCu_3Ti_4O_{12}$ powders prepared by egg white solution route: synthesis, characterization and its giant dielectric properties, Appl. Phys. A 91 (2008) 87–95.
[32] L. Liu, H. Fan, P. Fang, X. Chen, Sol–gel derived $CaCu_3Ti_4O_{12}$ ceramics: synthesis, characterization and electrical properties, Mater. Res. Bull. 43 (2008) 1800–1807.
[33] L. Marchin, S. Guillemet-Fritsch, B. Durand, Soft chemistry synthesis of the perovskite $CaCu_3Ti_4O_{12}$, Prog. Solid State Chem. 36 (2007) 151–155.
[34] L.C. Kretly, A.F.L. Almeida, R.S. Oliveira, J.M. Sasaki, A.S.B. Sombra, Electrical and optical properties of $CaCu_3Ti_4O_{12}$ substrates for

microwave devices and antennas Microw, Opt. Technol. Lett. 39 (2003) 145–150.
[35] J.-G. Li, T. Ishigaki, X.D. Sun, Anatase, brookite, and rutile nanocrystals via redox reactions under mild hydrothermal conditions: phase-selective synthesis and physicochemical properties, J. Phys. Chem.C 111 (2007) 4969–4976.
[36] F. Amarala, M. Valente, L.C. Costa, Synthesis and characterization of calcium copper titanate obtained by ethylene diamine tetra acetic acid gel combustion, Mater. .Chem. Phys. 124 (2010) 580–586.
[37] L. He, J.B. Neaton, M.H. Cohen, D. Vanderbilt, First-principles study of the structure and lattice dielectric response of $CaCu_3Ti_4O_{12}$, Phys. Rev. B 65 (2002) 214112–214123.
[38] D. Valim, A.G.S. Filho, P.T.C. Freire, S.B. Fagan, A.P. Ayala, J. Filho Mendes, P.B.A. Fechine, A.S.B. Sombra, L. Gerward, Raman scattering and x-ray diffraction studies of polycrystalline $CaCu_3Ti_4O_{12}$ under high-pressure, Phys. Rev. B 70 (2004) 1321031–1321034.
[39] P. Kubelka, F. Munk, Ein beitrag zur optik des farbanstriche, Z. Tech. Phys. 12 (1931) 593–601.
[40] D.L. Wood, J. Tauc, Weak absorption tails in amorphous semiconductors, Phys. Rev. B. 5 (1972) 3144–3151.
[41] Ch Kant, T. Rudolf, F. Mayr, S. Krohns, P. Lunkenheimer, S.G. Ebbinghaus, A. Loidl, Broadband dielectric response of $CaCu_3Ti_4O_{12}$: from dc to the electronic transition regime, Phys. Rev. B. 77 (2008) 045131–045134.
[42] L.S. Cavalcante, M.F.C. Gurgel, E.C. Paris, A.Z. Simões, M.R. Joya, J.A. Varela, P.S. Pizani, E. Longo, Combined experimental and theoretical investigations of the photoluminescent behavior of Ba(Ti,Zr)O3 thin films, Acta Mater. 55 (2007) 6416–6426.
[43] C. Laulhé, F. Hippert, J. Kreisel, M. Maglione, A. Simon, J.L. Hazemann., V. Nassif, EXAFS study of lead-free relaxor ferroelectric $BaTi_{1-x}Zr_xO_3$ at the Zr K edge, Phys. Rev. B 74 (2006) 014106.
[44] Q.G. Chi, L. Gao, X. Wanga, J.Q. Lin, J. Sun, Q.Q. Lei, Effects of Zr doping on the microstructures and dielectric properties of $CaCu_3Ti_4O_{12}$ ceramics, J. Alloy. Compd. 559 (2013) 45–48.
[45] P.R. Lucena, E.R. Leite, F.M. Pontes, E. Longo, P.S. Pizani, J.A. Varela, Intense and broad photoluminescence at room temperature in structurally disordered $Ba[Zr_{0.25}Ti_{0.75}]O_3$ powders: an experimental/theoretical correlation, J. Solid State Chem. 179 (2006) 3971–4002.
[46] F.A. Kroger, H.J. Vink, in: F. Seitz, D. Turnbull (Eds.), Solid State Physics, 3rd ed., Academic Press, New York, 1956, p. 307.
[47] L.S. Cavalcante, M.F.C. Gurgel, A.Z. Simões, E. Longo, J.A. Varela, M.R. Joya, P.S. Pizani, Intense visible photoluminescence in $Ba(Zr_{0.25}Ti_{0.75})O_3$ thin films, Appl. Phys. Lett. 90 (2007) 011901.
[48] R. Parra, E. Joanni, J.W.M. Espinosa, R. Tararam, M. Cilense, P.R. Bueno, J.A. Varela, E. Longo, Photoluminescent $CaCu_3Ti_4O_{12}$-based thin films synthesized by a sol–gel method, J. Am. Ceram. Soc. 91 (2008) 4162–4164.